



Contents lists available at ScienceDirect

Vision Research

journal homepage: www.elsevier.com/locate/visres

Li and Atick's theory of efficient binocular coding: A tutorial and mini-review

Keith May^{a,*}, Li Zhaoping^b

^a Department of Psychology, University of Essex, UK

^b Max Planck Institute for Biological Cybernetics, University of Tübingen, Germany

This article is published in Vision Research in 2022, in volume 201, 107950, <https://www.sciencedirect.com/science/article/abs/pii/S0042698921001863?via%3Dihub>

ARTICLE INFO

Keywords:

Binocular vision
Efficient coding
Theoretical neuroscience

ABSTRACT

Li and Atick (Network: Computation in Neural Systems 5 (1994) 157–174) presented a theory of efficient binocular encoding that explains a number of experimental findings. A binocular neuron is conventionally described in terms of two channels: the left and right eyes. Li and Atick's theory instead describes the neuron in terms of two alternative channels: the binocular sum and difference. The advantage of the latter description is that, unlike the left and right eye channels, the summation and differencing channels are usually uncorrelated; this means that each channel can be optimised independently of the other. The theory shows how to derive optimal receptive fields for the binocular summation and differencing channels; from these, it is easy to derive the neuron's optimal left and right eye receptive fields. The functional reality of the summation and differencing channels is demonstrated by a series of adaptation studies that confirm some counterintuitive predictions of the theory. Here we provide an accessible account of the theory, and review the evidence supporting it.

1. A generic linear neuronal model

1.1. The standard linear model of a binocular neuron

The standard linear model of a binocular simple cell (e.g. Ohzawa & Freeman, 1986) has two receptive fields, $K_L(x)$ and $K_R(x)$ for, respectively, the left and right eyes, where x is spatial position. These receptive fields give the sensitivity of the neuron as functions of spatial position in the two retinal images. If the left and right eye images (as functions of spatial position) are $S_L(x)$ and $S_R(x)$, then the output, O , of the linear neuron is given by

$$O = \sum_x K_R(x)S_R(x) + K_L(x)S_L(x). \quad (1)$$

Positive and negative regions of the receptive fields represent, respectively, “on” and “off” regions; positive and negative regions of the image signals represent, respectively, luminances above and below the mean. O in Eq. (1) represents the output of the linear spatial summation process carried out by the cell, which can be positive or negative. To obtain the overt spike rate from O , we subtract a threshold ≥ 0 , and then set all negative values to zero (Ohzawa & Freeman, 1986). For mathematical simplicity, in this article we only work with O , the linear part of the neuron's response.

1.2. A different description of the same standard model neuron

We now present a different description of the same model neuron; this description is equivalent to the previous one – each description can be derived from the other. Instead of describing the neuron in terms of its sensitivity to the left and right eye images, we can describe it in terms of its sensitivity to the sum of the left and right images (S_+) and the difference between the left and right images (S_-), where

$$S_+(x) = \frac{S_R(x) + S_L(x)}{\sqrt{2}} \quad (2)$$

$$S_-(x) = \frac{S_R(x) - S_L(x)}{\sqrt{2}}. \quad (3)$$

The division by $\sqrt{2}$ is just to keep the total signal power of S_+ and S_- the same as that for S_L and S_R . We can define receptive field profiles $K_+(x)$ and $K_-(x)$ that allow us to determine the neuron's output from the sum and difference images:

$$O = \sum_x K_+(x)S_+(x) + K_-(x)S_-(x). \quad (4)$$

* Corresponding author at: Department of Psychology, University of Essex, Wivenhoe Park, Colchester CO4 3SQ, UK.

E-mail address: keith.may@essex.ac.uk (K. May).

<https://doi.org/10.1016/j.visres.2021.08.005>

Received 14 October 2020; Received in revised form 10 August 2021; Accepted 19 August 2021

0042-6989/© 2021 Elsevier Ltd. All rights reserved.

We are *not* proposing that the visual system necessarily adds and subtracts the two eyes' images to produce signals $S_+(x)$ and $S_-(x)$ before applying receptive fields $K_+(x)$ and $K_-(x)$. Eqs. (1) and (4) both describe exactly the *same* model neuron, each providing a different, but equally valid way of calculating its output. Eq. (1) comes closer to describing how this model would actually be implemented in the brain; Eq. (4) gives an alternative way to calculate the model neuron's response, which turns out to be more useful when deriving the optimal receptive fields. We can ensure that Eq. (4) gives the same output as Eq. (1) by starting with the premise that the outputs from the two equations are equal and then deriving $K_+(x)$ and $K_-(x)$ from that premise. Using Eqs. (2) and (3) and to substitute for $S_+(x)$ and $S_-(x)$ in Eq. (4), and then rearranging, we have

$$O = \sum_x \frac{K_+(x) + K_-(x)}{\sqrt{2}} S_R(x) + \frac{K_+(x) - K_-(x)}{\sqrt{2}} S_L(x). \quad (5)$$

Eq. (5) has the same form as Eq. (1), with

$$K_R(x) = \frac{K_+(x) + K_-(x)}{\sqrt{2}} \quad (6)$$

$$K_L(x) = \frac{K_+(x) - K_-(x)}{\sqrt{2}}. \quad (7)$$

Eq. (4) describes the neuron's output in terms of its sensitivity to two "channels": a binocular summation channel and a binocular differencing channel. Alternatively, Eq. (1) describes the same neuron's response in more conventional terms, i.e. in terms of its sensitivity to the left and right eyes' images. To derive the optimal binocular code, we derive the optimal receptive field profiles for the summation and differencing channels, and then use Eqs. (6) and (7) to obtain the optimal receptive field profiles for the left and right eyes.

2. Deriving the optimal binocular code

The theory described in this article was first presented by Li and Atick (1994), and further expounded by Zhaoping (2014); please note that the names "Li" and "Zhaoping" in these citations both refer to Li Zhaoping, the second author of this article.

Deriving the optimal binocular code involves finding the best trade-off between cost (energy usage) and benefit (information transfer). The measure of information that we use is "mutual information", the information about the external sensory signal contained in the neuronal signal. Supplementary Appendix A explains how mutual information is defined and quantified, but the rest of this article can be understood without referring to this appendix.

2.1. Encoding the sensory signal

Instead of considering the signal to be a whole 2-dimensional (2D) image in each eye, we will begin by considering a single point at the same location in each eye. This will allow us to determine the optimal sensitivity to each eye's signal, but ignores the spatial aspects of the receptive field. We will then extend the exposition to full 2D images and receptive fields in Section 3. As a further simplification, we will consider only luminance, not spectral wavelength. So the sensory input signal is represented by two values, S_L and S_R , the luminances of a pair of points with the same location in the left and right eye retinal images. For mathematical simplicity, we assume that all signals and noise have zero-mean Gaussian distributions; thus, the luminance signal is normalised by subtracting the mean, so the signal can take positive or negative values.

We will often find it convenient to represent the sensory input signal using a column vector, \mathbf{S} , given by

$$\mathbf{S} = \begin{pmatrix} S_L \\ S_R \end{pmatrix}. \quad (8)$$

In the text, we will sometimes write \mathbf{S} as $(S_L, S_R)^T$, and similarly for other vectors; the superscript T means "transpose", which converts the row vector to a column vector. We use this for notational convenience because, although \mathbf{S} is a column vector, row vectors take up less space in the text.

We assume that this sensory signal is corrupted by additive sensory noise, \mathbf{N} , given by

$$\mathbf{N} = \begin{pmatrix} N_L \\ N_R \end{pmatrix}, \quad (9)$$

to give a noisy sensory signal, \mathbf{S}' :

$$\mathbf{S}' = \mathbf{S} + \mathbf{N} = \begin{pmatrix} S_L + N_L \\ S_R + N_R \end{pmatrix} = \begin{pmatrix} S'_L \\ S'_R \end{pmatrix}. \quad (10)$$

To maintain the information in this 2-element vector, we need to encode it using at least two output channels, whose values are labelled O_1 and O_2 :

$$\mathbf{O} = \begin{pmatrix} O_1 \\ O_2 \end{pmatrix}. \quad (11)$$

We assume that the output of each channel, O_i , is a linear function of the two eyes' noisy sensory signals, plus added noise. The response of channel 1 is given by

$$O_1 = K_{1L}S'_L + K_{1R}S'_R + (N_O)_1, \quad (12)$$

where K_{1L} and K_{1R} are the sensitivities of channel 1 to the left and right eyes' signals, respectively (Zhaoping, 2014, Equation 3.103); $(N_O)_1$ is a noise sample added to the output of channel 1, due to noise in the encoding process. Similarly,

$$O_2 = K_{2L}S'_L + K_{2R}S'_R + (N_O)_2. \quad (13)$$

Eqs. (12) and (13) are analogous to Eq. (1), except that the images and receptive fields have been reduced from 2D images to single, scalar numbers, and encoding noise has been added to the output.

Eqs. (12) and (13) can be expressed in matrix form as follows (Zhaoping, 2014, Equation 3.102):

$$\begin{pmatrix} O_1 \\ O_2 \end{pmatrix} = \begin{pmatrix} K_{1L} & K_{1R} \\ K_{2L} & K_{2R} \end{pmatrix} \begin{pmatrix} S'_L \\ S'_R \end{pmatrix} + \begin{pmatrix} (N_O)_1 \\ (N_O)_2 \end{pmatrix}, \quad (14)$$

or more compactly:

$$\mathbf{O} = \mathbf{K}\mathbf{S}' + \mathbf{N}_O. \quad (15)$$

The goal of efficient coding is to find an encoding matrix, \mathbf{K} , that gives the best trade-off between information and cost.

2.2. Finding the optimal encoding matrix

Zhaoping (2014) uses the output variance as the measure of cost, because the energy usage will increase with increasing variance (Zhaoping, 2014, Section 3.2.2.3). Because we assume the signals to have zero mean, the variance of output i is simply $\langle O_i^2 \rangle$, where $\langle y \rangle$ is the mean of y . The optimal matrix, \mathbf{K} , is the one that minimises the loss function,

$$E(\mathbf{K}) = \left(\sum_{i=1,2} \langle O_i^2 \rangle \right) - \lambda I(\mathbf{O}; \mathbf{S}), \quad (16)$$

where $I(\mathbf{O}; \mathbf{S})$ is the mutual information between the sensory input signal, \mathbf{S} , and the neuronal output, \mathbf{O} . Good encoding matrices will be those that give a low total energy consumption, $\sum_{i=1,2} \langle O_i^2 \rangle$, or a high mutual information, or both. The free parameter, λ , quantifies the importance of information relative to energy usage: it tells us the maximum amount of energy we are prepared to expend per bit of information.

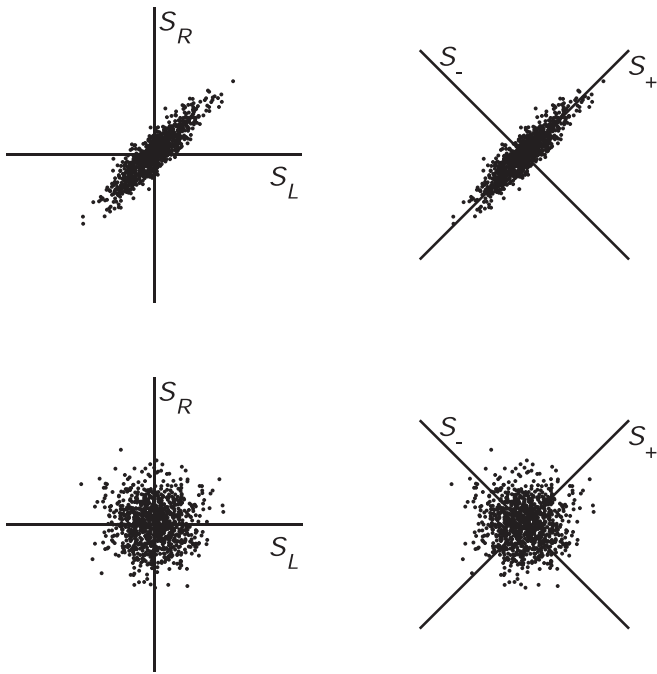


Fig. 1. Idealised distributions of signal values in the left and right eyes. In the left column, each point plots the luminance of a point in the left eye (S_L) against the luminance at the same location in the right eye (S_R); each eye's signal is a Gaussian distribution with the same variance. In the top row, the correlation between the left and right eyes is 0.9; in the bottom row, the correlation is zero. The right column shows the same distributions, but plotted on axes representing the binocular sum (S_+) and difference (S_-), which are rotated by 45° with respect to the S_L and S_R axes. When the two eyes' signals are correlated (top row), $\langle S_+^2 \rangle > \langle S_-^2 \rangle$; when the two eyes' signals are uncorrelated (bottom row), $\langle S_+^2 \rangle = \langle S_-^2 \rangle$. In both cases, the S_+ and S_- signals are uncorrelated.

In general, the two elements of the sensory input signal $\mathbf{S} = (S_L, S_R)^T$ are correlated, because the left eye's image is similar to the right eye's image (as in the top-left panel of Fig. 1): each eye's signal carries information about the other. This makes it difficult to minimise the loss function, because any change in the sensitivity to one eye's signal can influence the amount of additional information provided by the other eye. Imagine that, instead, we had a signal $\mathbf{S} = (S_1, S_2)^T$ in which S_1 and S_2 were uncorrelated; and imagine further that O_1 provided information only about S_1 , and O_2 provided information only about S_2 . Then O_1 provides $I(O_1; S_1)$ bits of information about the signal and O_2 provides

$$\begin{pmatrix} S'_+ \\ S'_- \end{pmatrix} = \mathbf{K}_O \begin{pmatrix} S'_L \\ S'_R \end{pmatrix} = \frac{1}{\sqrt{2}} \begin{pmatrix} S'_R + S'_L \\ S'_R - S'_L \end{pmatrix} = \frac{1}{\sqrt{2}} \begin{pmatrix} S_R + S_L \\ S_R - S_L \end{pmatrix} + \frac{1}{\sqrt{2}} \begin{pmatrix} N_R + N_L \\ N_R - N_L \end{pmatrix} = \begin{pmatrix} S_+ \\ S_- \end{pmatrix} + \begin{pmatrix} N_+ \\ N_- \end{pmatrix} \quad (22)$$

$I(O_2; S_2)$ bits about the signal. Because there is no overlap between the information provided by O_1 and O_2 , the total information given by O_1 and O_2 together is simply the sum of the information that each provides individually:

$$I(\mathbf{O}; \mathbf{S}) = \sum_{i=1,2} I(O_i; S_i). \quad (17)$$

Using Eq. (17) to substitute for $I(\mathbf{O}; \mathbf{S})$ in Eq. (16), we have

$$E(\mathbf{K}) = \sum_{i=1,2} E_i(\mathbf{K}), \quad (18)$$

where

$$E_i(\mathbf{K}) = \langle O_i^2 \rangle - \lambda I(O_i; S_i). \quad (19)$$

$E(\mathbf{K})$ is therefore a sum of terms, $E_i(\mathbf{K})$, one for each output channel. Each channel's output, O_i , carries information only about the corresponding input element S_i , and no information about the other input element; because of this, any change that we make to one channel has no effect on the other channel's $E_i(\mathbf{K})$ term, so we can minimise $E(\mathbf{K})$ by minimising each channel's $E_i(\mathbf{K})$ term independently of the others; this makes the process quite straightforward. Thus, the first step in finding the optimal \mathbf{K} is to apply an information-preserving linear transformation (matrix \mathbf{K}_O – Eq. (21)) that transforms the correlated sensory input signal, $(S_L, S_R)^T$, into a decorrelated signal, $(S_1, S_2)^T$; then the loss function can be written in the form given in Eq. (18). The second step is to find a linear transformation that minimises each channel's term in the loss function; because each channel is being optimised independently of the other, and the signals are single scalar values, this linear transformation is a simple gain control in each channel (matrix \mathbf{g} – Eq. (28)). Finally, there is a third step in which O_1 and O_2 are multiplexed across two further channels to produce an encoding scheme that is equally optimal in terms of the loss function, but can reduce the amount of neural wiring required to implement it. Conceptually, the process consists of three linear transformations, as just described. However, there is no need for these three stages to be carried out separately in the brain: they could all be cascaded into a single linear transformation. In the next three subsections, we outline these three stages.

2.2.1. Step 1: Decorrelation

Assuming the inputs to the two eyes have the same variance, so $\langle S_L^2 \rangle = \langle S_R^2 \rangle$, we can decorrelate the signals by rotating the coordinate axes by 45° (positive angles give anticlockwise rotations; negative angles give clockwise rotations) – see Fig. 1. Rotating the axes by θ is equivalent to rotating the points about the origin by $-\theta$. This can be achieved by multiplying the signal vector by a standard rotation matrix,

$$\begin{pmatrix} \cos(-\theta) & -\sin(-\theta) \\ \sin(-\theta) & \cos(-\theta) \end{pmatrix} = \begin{pmatrix} \cos(\theta) & \sin(\theta) \\ -\sin(\theta) & \cos(\theta) \end{pmatrix}. \quad (20)$$

With $\theta = 45^\circ$, we call this matrix \mathbf{K}_O :

$$\mathbf{K}_O = \begin{pmatrix} \cos(45) & \sin(45) \\ -\sin(45) & \cos(45) \end{pmatrix} = \frac{1}{\sqrt{2}} \begin{pmatrix} 1 & 1 \\ -1 & 1 \end{pmatrix}. \quad (21)$$

Using \mathbf{K}_O , we can transform the noisy sensory signal $\mathbf{S}' = (S'_L, S'_R)^T$ to a decorrelated signal $(S'_+, S'_-)^T$:

where

$$S_+ = (S_R + S_L)/\sqrt{2} \quad (23)$$

$$S_- = (S_R - S_L)/\sqrt{2} \quad (24)$$

$$N_+ = (N_R + N_L)/\sqrt{2} \quad (25)$$

$$N_- = (N_R - N_L)/\sqrt{2}. \quad (26)$$

Note that we use the subscripts $+$ and $-$ to refer to the decorrelated

signals, rather than the more general subscripts 1 and 2 in the previous sections. This is because, in this particular case, the decorrelation transform creates a summation channel, S_+ , which adds the two eyes' sensory signals together, and a differencing channel, S_- , which subtracts one eye's signal from the other. The effect of this rotation of the coordinate axes is illustrated in Fig. 1. In these new coordinate axes, the signals are now decorrelated.

Transforming the correlated signal $(S'_L, S'_R)^T$ to the decorrelated signal $(S'_+, S'_-)^T$ does not change the amount of information that we have about the original sensory signal, $(S_L, S_R)^T$. This is because the transformation is completely reversible – given $(S'_+, S'_-)^T$, we can rotate the axes back to find $(S'_L, S'_R)^T$, and vice-versa, so $(S'_L, S'_R)^T$ and $(S'_+, S'_-)^T$ are equally informative about the original sensory signal, $(S_L, S_R)^T$. More formally, we can say that the mutual information between $(S_L, S_R)^T$ and $(S'_L, S'_R)^T$ is the same as the mutual information between $(S_L, S_R)^T$ and $(S'_+, S'_-)^T$:

$$I\left((S'_+, S'_-)^T; (S_L, S_R)^T\right) = I\left((S'_L, S'_R)^T; (S_L, S_R)^T\right). \quad (27)$$

So, if $(S'_L, S'_R)^T$ or $(S'_+, S'_-)^T$ were the output, \mathbf{O} , then the second term in the loss function (Eq. (16)), i.e. $\lambda I(\mathbf{O}; \mathbf{S})$, would be unchanged by this decorrelation. Furthermore, the first term in the loss function is the sum of the variances of the output neurons, and it can be shown that this, too, is unchanged by the rotation of the coordinate axes (Zhaoping, 2014, p. 99). Thus, neither term in the loss function is changed by the rotation, and so the $(S'_+, S'_-)^T$ encoding scheme is no more efficient by this measure than the $(S'_L, S'_R)^T$ scheme. It is true that $(S'_+, S'_-)^T$ is less *redundant* than $(S'_L, S'_R)^T$ (Attneave, 1954; Barlow, 1961; Barlow, 2001), because, unlike $(S'_L, S'_R)^T$, there is no overlap in the information in the two elements of $(S'_+, S'_-)^T$. However, in Li and Atick's theory, the decorrelation itself does not increase the efficiency – it merely provides a conceptual stage that allows straightforward derivation of the optimal \mathbf{K} through simple gain control in each channel: because the channels are uncorrelated, the optimal gain in each channel can be derived independently of the other channel.

2.2.2. Step 2: Gain control

We can apply gain control to the transformed signal, $(S'_+, S'_-)^T$, by applying a diagonal gain control matrix, \mathbf{g} , given by

$$\mathbf{g} = \begin{pmatrix} g_+ & 0 \\ 0 & g_- \end{pmatrix}. \quad (28)$$

When the gain values, g_+ and g_- , have been optimised, the optimal encoding matrix, \mathbf{K} , is given by

$$\mathbf{K} = \mathbf{g}\mathbf{K}_0 = \frac{1}{\sqrt{2}} \begin{pmatrix} g_+ & g_+ \\ -g_- & g_- \end{pmatrix}. \quad (29)$$

Then, by expanding Eq. (15), we have

$$\begin{pmatrix} O_+ \\ O_- \end{pmatrix} = \frac{1}{\sqrt{2}} \begin{pmatrix} g_+ & g_+ \\ -g_- & g_- \end{pmatrix} \begin{pmatrix} S_L + N_L \\ S_R + N_R \end{pmatrix} + \begin{pmatrix} (N_O)_+ \\ (N_O)_- \end{pmatrix} \quad (30)$$

$$= \begin{pmatrix} \frac{g_+(S_R + S_L) + g_+(N_R + N_L)}{\sqrt{2}} + (N_O)_+ \\ \frac{g_-(S_R - S_L) + g_-(N_R - N_L)}{\sqrt{2}} + (N_O)_- \end{pmatrix} \quad (31)$$

$$= \begin{pmatrix} g_+S_+ + g_+N_+ + (N_O)_+ \\ g_-S_- + g_-N_- + (N_O)_- \end{pmatrix}. \quad (32)$$

We now show how to calculate the optimal gain in each channel. Let

us assume that the sensory noise samples, N_L and N_R , are uncorrelated and both sampled from a Gaussian distribution with mean zero and variance $\langle N^2 \rangle$: then it can be shown that noise samples N_+ and N_- are also uncorrelated, and sampled from the same distribution (Zhaoping, 2014, Equation 3.111). We also assume that the encoding noise samples, $(N_O)_+$ and $(N_O)_-$, are both sampled from a zero-mean Gaussian distribution with variance $\langle N_O^2 \rangle$. Thus, each output, O_i , is the sum of three independent Gaussian random variables. Since the variances of summed independent signals add, the output variance, $\sigma_{O_i}^2$, is given by

$$\sigma_{O_i}^2 = \langle O_i^2 \rangle = g_i^2 (\langle S_i^2 \rangle + \langle N^2 \rangle) + \langle N_O^2 \rangle. \quad (33)$$

Similarly, the total noise variance, σ_N^2 , for each channel is given by

$$\sigma_N^2 = g_i^2 \langle N^2 \rangle + \langle N_O^2 \rangle. \quad (34)$$

For Gaussian-distributed signals and noise, the mutual information between the input and output is given by (Zhaoping, 2014, Equation 3.25)

$$I(O_i; S_i) = \log_2 \frac{\sigma_{O_i}}{\sigma_N} \quad (35)$$

$$= \frac{1}{2} \log_2 \frac{\sigma_{O_i}^2}{\sigma_N^2} \quad (36)$$

$$= \frac{1}{2} \log_2 \frac{g_i^2 (\langle S_i^2 \rangle + \langle N^2 \rangle) + \langle N_O^2 \rangle}{g_i^2 \langle N^2 \rangle + \langle N_O^2 \rangle}. \quad (37)$$

Using Eqs. (33) and (37) to substitute for $\langle O_i^2 \rangle$ and $I(O_i; S_i)$ in Eq. (19), we have

$$E_i(\mathbf{K}) = g_i^2 (\langle S_i^2 \rangle + \langle N^2 \rangle) + \langle N_O^2 \rangle - \frac{\lambda}{2} \log_2 \frac{g_i^2 (\langle S_i^2 \rangle + \langle N^2 \rangle) + \langle N_O^2 \rangle}{g_i^2 \langle N^2 \rangle + \langle N_O^2 \rangle}. \quad (38)$$

For each channel, i , the optimal gain, g_i , is that which minimises $E_i(\mathbf{K})$. This is found by differentiating Eq. (38) with respect to g_i^2 , setting the result to zero, and solving for g_i^2 . The derivative of $E_i(\mathbf{K})$ is given by

$$\frac{dE_i(\mathbf{K})}{d(g_i^2)} = \langle S_i^2 \rangle + \langle N^2 \rangle - \frac{1}{2 \ln 2} \times \frac{\lambda \langle N_O^2 \rangle \langle S_i^2 \rangle}{(g_i^2)^2 \langle N^2 \rangle (\langle S_i^2 \rangle + \langle N^2 \rangle) + g_i^2 \langle N_O^2 \rangle (\langle S_i^2 \rangle + 2 \langle N^2 \rangle) + \langle N_O^2 \rangle^2}. \quad (39)$$

Setting $dE_i(\mathbf{K})/d(g_i^2)$ to zero gives

$$a(g_i^2)^2 + bg_i^2 + c = 0 \quad (40)$$

where

$$a = \langle N^2 \rangle (\langle S_i^2 \rangle + \langle N^2 \rangle) \quad (41)$$

$$b = \langle N_O^2 \rangle (\langle S_i^2 \rangle + 2 \langle N^2 \rangle) \quad (42)$$

$$c = \langle N_O^2 \rangle^2 - \frac{\lambda \langle N_O^2 \rangle \langle S_i^2 \rangle}{2 \ln 2 (\langle S_i^2 \rangle + \langle N^2 \rangle)}. \quad (43)$$

Using the quadratic formula to solve Eq. (40) for g_i^2 , we find that the optimal gain is given by

$$g_i^2 = \frac{\langle N_O^2 \rangle}{\langle N^2 \rangle} (F_{\text{smoothing}} \times F_{\text{decorrelation}} - 1) \quad (44)$$

where

$$F_{\text{smoothing}} = \left(1 + \frac{\langle N^2 \rangle}{\langle S_i^2 \rangle}\right)^{-1} \quad (45)$$

$$F_{\text{decorrelation}} = \frac{1}{2} + \frac{1}{2} \sqrt{1 + \frac{2\lambda}{\langle N_o^2 \rangle \ln 2} \times \frac{\langle N^2 \rangle}{\langle S_i^2 \rangle}}. \quad (46)$$

Note that, when λ is low, Eq. (44) can produce negative, i.e. impossible, values for g_i^2 ; in this case, the optimal achievable value for g_i^2 will be zero, indicating that any of the information in the sensory signal would cost more in energy terms than we are prepared to pay. Eqs. (44) to (46) are plotted in Fig. 2, each panel plotting a different set of parameter values. $F_{\text{smoothing}}$ increases with increasing ratio of signal to sensory noise, $\langle S_i^2 \rangle / \langle N^2 \rangle$, while $F_{\text{decorrelation}}$ does the opposite. At high signal-to-noise ratios (SNRs), $F_{\text{smoothing}}$ asymptotes to 1, so the gain is dominated by $F_{\text{decorrelation}}$: in this situation, the optimal gain varies inversely with the SNR; this approximately has the effect of whitening, i.e. making all outputs equally strong, which decorrelates the outputs (see the bottom row of Fig. 1), hence the name, $F_{\text{decorrelation}}$. At low SNRs, $F_{\text{smoothing}}$ and $F_{\text{decorrelation}}$ change in opposite directions with SNR, but $F_{\text{smoothing}}$ is steeper, so the optimal gain follows $F_{\text{smoothing}}$, increasing with the SNR; this has the effect of suppressing weak, noisy signals, i.e. smoothing out the noise, hence the name $F_{\text{smoothing}}$.

2.2.3. Step 3: Multiplexing

After steps 1 and 2, we have two channels: the summation channel, O_+ , which tells us about the sum of the two eyes' images, and the differencing channel, O_- , which tells us about the difference between them; the gain on each channel can be adjusted to optimise coding efficiency. The encoding process could stop there. However, the optimal code is not unique. In Section 2.2.1, we noted that rotating the

coordinate axes of the encoding scheme had no effect on either the total information or the sum of variances of the outputs, so both terms of the loss function (Eq. (16)) are unchanged. This is equally true after gain control: the coordinate axes can subsequently be rotated through any angle, to produce a new encoding scheme that is just as optimal as the one found in step 2. This can be achieved by multiplying by a further rotation matrix, $U(\theta)$, to rotate the axes about an angle θ :

$$U(\theta) = \begin{pmatrix} \cos \theta & \sin \theta \\ -\sin \theta & \cos \theta \end{pmatrix}. \quad (47)$$

The full encoding matrix, K , is then given by

$$K = U(\theta)gK_o = \frac{1}{\sqrt{2}} \begin{pmatrix} \cos \theta & \sin \theta \\ -\sin \theta & \cos \theta \end{pmatrix} \begin{pmatrix} g_+ & 0 \\ 0 & g_- \end{pmatrix} \begin{pmatrix} 1 & 1 \\ -1 & 1 \end{pmatrix}, \quad (48)$$

with θ a free parameter, and the optimal g_+ and g_- determined by Eq. (44). For all values of θ except integer multiples of 90° , the summation and differencing channels are multiplexed across the two output channels (so both channels carry information about the sum and difference signals, S_+ and S_-).

Although any value of θ is equally optimal in minimising the loss function (Eq. (16)), Li and Atick (1994) assume a value of $\theta = -45^\circ$. In this case, $U(\theta)$ is the inverse of K_o , as it rotates the axes 45° in the opposite direction to K_o . Li and Atick (1994) note that this results in the smallest overall change to the input, i.e. it minimises $\sum_i (O_i - S_i)^2$ (see Zhaoping, 2014, Box 3.1). This may minimise the amount of neural wiring involved in transforming the signal, conferring an additional advantage that is not taken into account by the loss function of Eq. (16). With $\theta = -45^\circ$, Eq. (48) simplifies to

$$K = \frac{1}{2} \begin{pmatrix} g_+ + g_- & g_+ - g_- \\ g_+ - g_- & g_+ + g_- \end{pmatrix}. \quad (49)$$

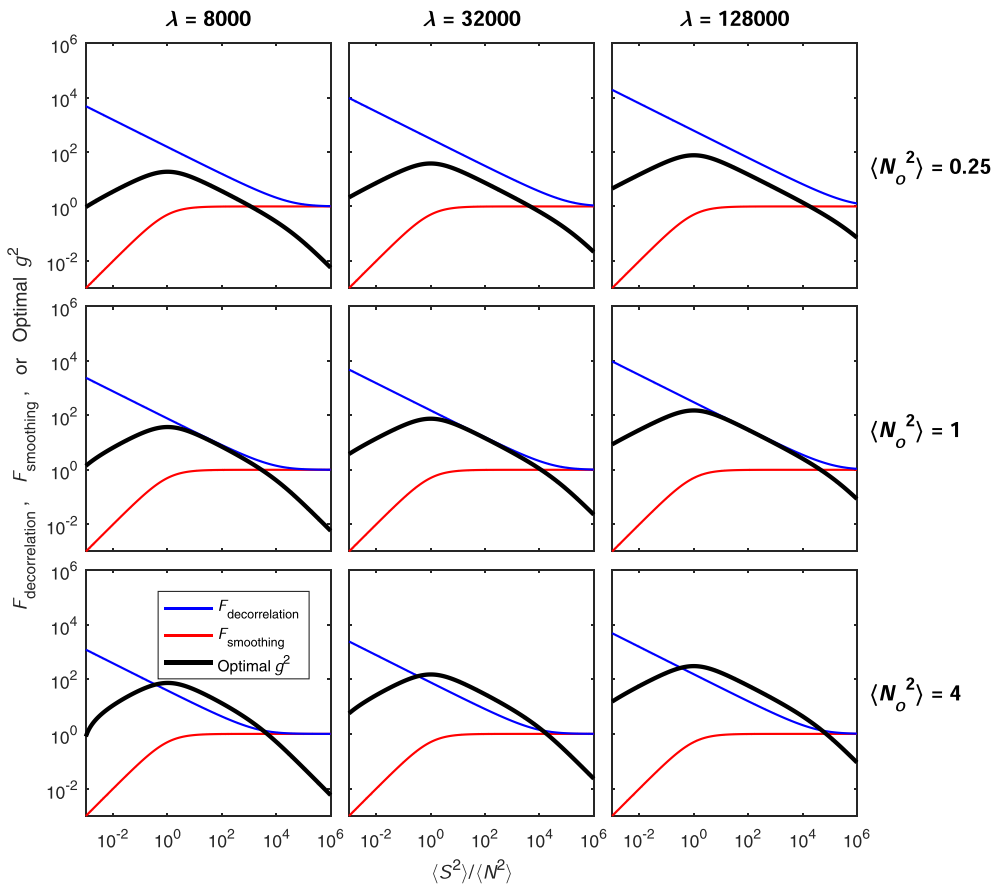


Fig. 2. Optimal gain. Each panel shows $F_{\text{decorrelation}}$, $F_{\text{smoothing}}$ and the optimal g^2 for a different combination of parameters λ and $\langle N_o^2 \rangle$. g^2 , $\langle N^2 \rangle$ and $\langle N_o^2 \rangle$ are specified in units of sensory noise variance, so $\langle N^2 \rangle = 1$ by definition. The red curve shows $F_{\text{smoothing}}$, which is the same in each panel. The blue curve shows $F_{\text{decorrelation}}$; this increases in height with increasing λ , and decreases in height with increasing $\langle N_o^2 \rangle$. Panels on the same diagonal (top left to bottom right) have the same $F_{\text{decorrelation}}$, because within a diagonal, $\lambda / \langle N_o^2 \rangle$ is constant. The optimal g^2 is given by Eq. (44).

If the two eyes' signals are already uncorrelated, then the binocular summation and differencing channels will have the same signal strength as each other (see Fig. 1), and thus the same optimal gain; in this case, we can let $g = g_+ = g_-$, giving

$$K = g \begin{pmatrix} 1 & 0 \\ 0 & 1 \end{pmatrix}. \quad (50)$$

Using Eq. (50) to substitute for K in Eq. (15), we have

$$\begin{pmatrix} O_1 \\ O_2 \end{pmatrix} = g \begin{pmatrix} S'_L \\ S'_R \end{pmatrix} + \begin{pmatrix} (N_o)_1 \\ (N_o)_2 \end{pmatrix}. \quad (51)$$

In this case, the optimal transform does nothing except change the gain. Multiplexing the summation and differencing channels using $U(-45^\circ)$ is particularly beneficial in this case, as it results in each output channel receiving its input from just one eye, eliminating the need for neural connections from both eyes.

In the more general case of $g_+ \neq g_-$, the output is found by using Eq. (49) to substitute for K in Eq. (15):

$$\begin{pmatrix} O_1 \\ O_2 \end{pmatrix} = \frac{1}{2} \begin{pmatrix} (g_+ + g_-)S'_L + (g_+ - g_-)S'_R \\ (g_+ - g_-)S'_L + (g_+ + g_-)S'_R \end{pmatrix} + \begin{pmatrix} (N_o)_1 \\ (N_o)_2 \end{pmatrix}. \quad (52)$$

Carrying out the matrix operations defined in Eq. (52), we obtain

$$O_1 = \frac{g_+ + g_-}{2} S'_L + \frac{g_+ - g_-}{2} S'_R + (N_o)_1 \quad (53)$$

$$O_2 = \frac{g_+ - g_-}{2} S'_L + \frac{g_+ + g_-}{2} S'_R + (N_o)_2. \quad (54)$$

Eqs. (53) and (54) tell us how to calculate the outputs of channels 1 and 2 from the left and right eye inputs. Each channel has the same pair of ocular sensitivities, i.e. $(g_+ + g_-)/2$ and $(g_+ - g_-)/2$, but they differ in which eye has which sensitivity.

It will be useful to present alternative equations that tell us how to calculate the channel outputs from the noisy sum and difference signals, S'_+ and S'_- . From Eq. (22), we obtain

$$S'_R = \frac{S'_+ + S'_-}{\sqrt{2}} \quad (55)$$

$$S'_L = \frac{S'_+ - S'_-}{\sqrt{2}}. \quad (56)$$

Using Eqs. (55) and (56) to substitute for S'_L and S'_R in Eqs. (53) and (54), we obtain

$$O_1 = \frac{g_+}{\sqrt{2}} S'_+ - \frac{g_-}{\sqrt{2}} S'_- + (N_o)_1 \quad (57)$$

$$O_2 = \frac{g_+}{\sqrt{2}} S'_+ + \frac{g_-}{\sqrt{2}} S'_- + (N_o)_2. \quad (58)$$

Eqs. (57) and (58) are not presenting a different model from Eqs. (53) and (54): instead, Eqs. (57) and (58) give us, the researchers, an alternative way to calculate the model's responses. The brain would still calculate the outputs from the left and right eye signals, as made explicit in Eqs. (53) and (54). Eqs. (57) and (58) show that using $U(-45^\circ)$ in the multiplexing step divides the summation and differencing channels equally between the two output channels: the two output channels both have a sensitivity of $g_+/\sqrt{2}$ to the summation signal, and both have a sensitivity of $g_-/\sqrt{2}$ to the difference signal.

2.3. Summary so far

This is a good point to take stock of what we have done, before moving on. The sensory input signal is a two-element vector, $\mathbf{S} = (S_L, S_R)^T$. During

the transduction process, this signal gets corrupted by additive sensory noise, to give a noisy sensory signal, $\mathbf{S}' = (S_L + N_L, S_R + N_R)^T$ (Eq. (10)). In transforming \mathbf{S}' to an efficient code, \mathbf{O} , the visual system applies a linear transformation to give an output signal, $\mathbf{O} = \mathbf{K}\mathbf{S}' + \mathbf{N}_o$ (Eq. (15)), where \mathbf{N}_o is encoding noise (a different source of noise from the sensory noise). The optimal encoding matrix, \mathbf{K} , is given by Eq. (49), with the gain values, g_+ and g_- , determined by Eq. (44). This linear transformation can be conceptually divided into a series of three steps, represented by the three matrices in Eq. (48): (1) a decorrelation that converts the left and right eye signals to binocular sum and difference signals; (2) gain control, which finds the optimal trade-off between energy usage and information transfer within the summation channel and within the differencing channel; (3) multiplexing the summation and differencing channels across the two output channels; this transformation preserves both energy consumption and information, and is therefore just as optimal as the encoding scheme obtained in step 2. The purpose of the decorrelation in step 1 is to ensure that the two channels do not share information, so that, in step 2, the whole system can be optimised by optimising each channel independently of the other. Step 3 minimises the difference between the input and output signals, which can reduce the amount of neural wiring needed to implement the process. Step 3 delivers two output channels, each of which has sensitivity $g_+/\sqrt{2}$ to the summation signal and sensitivity $g_-/\sqrt{2}$ to the difference signal (Eqs. (57) and (58)).

3. Deriving the receptive field profiles for a neuron

So far, we have ignored the spatial aspects of the stimuli, just deriving each output channel's sensitivity. We will now expand our analysis to include the spatial receptive fields. We will consider the output channel to be a linear neuron, as defined in Section 1. To begin with, we extend Eq. (4) to include both sensory and encoding noise:

$$O = \left(\sum_x K_+(x) S'_+(x) + K_-(x) S'_-(x) \right) + N_o. \quad (59)$$

We will take $K_+(x)$ and $K_-(x)$ to be Gabor functions, whose 1-dimensional cross-section is given by

$$K(x) = sG(x)\cos(2\pi fx + \phi), \quad (60)$$

where s is the sensitivity, f is the neuron's preferred spatial frequency, ϕ is the carrier phase, and $G(x)$ is a Gaussian envelope, given by

$$G(x) = \exp\left(-\frac{x^2}{2\sigma^2}\right). \quad (61)$$

σ is the standard deviation of the Gaussian envelope, which controls its width. The centre of the envelope is defined as spatial position $x = 0$.

As noted above, the neuron's sensitivity to the binocular sum and binocular difference are $g_+/\sqrt{2}$ and $g_-/\sqrt{2}$, respectively. This gives the following receptive fields:

$$K_+(x) = \frac{g_+}{\sqrt{2}} G(x)\cos(2\pi fx + \phi_+) \quad (62)$$

$$K_-(x) = \frac{g_-}{\sqrt{2}} G(x)\cos(2\pi fx + \phi_-). \quad (63)$$

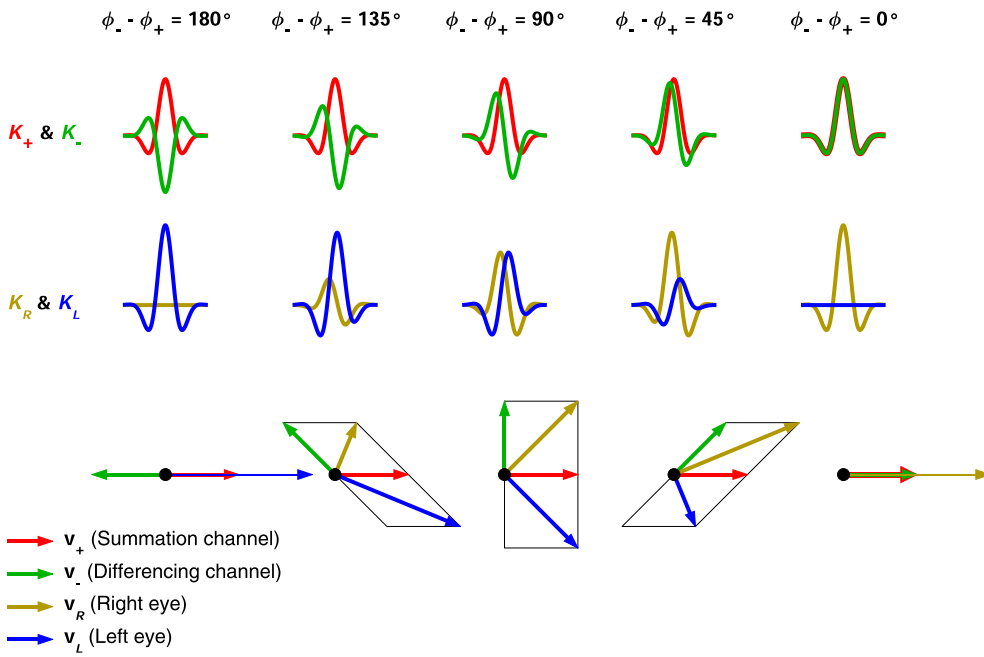


Fig. 3. Representations of the receptive fields with $g_+/g_- = 1$. Each column shows a different phase disparity, $\phi_- - \phi_+$, between the summation and differencing channels. In these examples, ϕ_+ is always zero. The top row shows $K_+(x)$ in red, and $K_-(x)$ in green; the middle row shows $K_R(x)$ in yellow, and $K_L(x)$ in blue. The bottom row shows the vector representation of these receptive fields. Each vector is coloured to match the colour of the corresponding receptive field profile in the rows above. The angle of each vector represents the phase of the corresponding receptive field (measured anticlockwise from 3 o'clock). The lengths of the vectors v_+ and v_- represent $g_+/\sqrt{2}$ and $g_-/\sqrt{2}$, respectively. The lengths of the vectors v_L and v_R represent g_L and g_R , respectively. Thus, the lengths of v_+ and v_- give the neuron's sensitivities to the summation and difference images, whereas the lengths of v_L and v_R are larger than the neuron's sensitivities to the left and right eye images, by a factor of $\sqrt{2}$. v_R is the sum of vectors v_+ and v_- , while v_L is the difference, $v_+ - v_-$. When $g_+/g_- = 1$, as in this figure, v_+ and v_- are the same length. Because of this, the parallelo-

grams formed by the vector addition and subtraction are identical rhombuses, so the diagonals (on which v_L and v_R lie) are orthogonal. This forces the magnitude of the neuron's preferred binocular phase disparity, $|\phi_L - \phi_R|$, to be equal to 90° in all cases, regardless of the values of ϕ_+ or ϕ_- , apart from the degenerate cases of $\phi_- - \phi_+ = 0^\circ$ or 180° , when the neuron is completely monocular, so the binocular phase disparity cannot be defined.

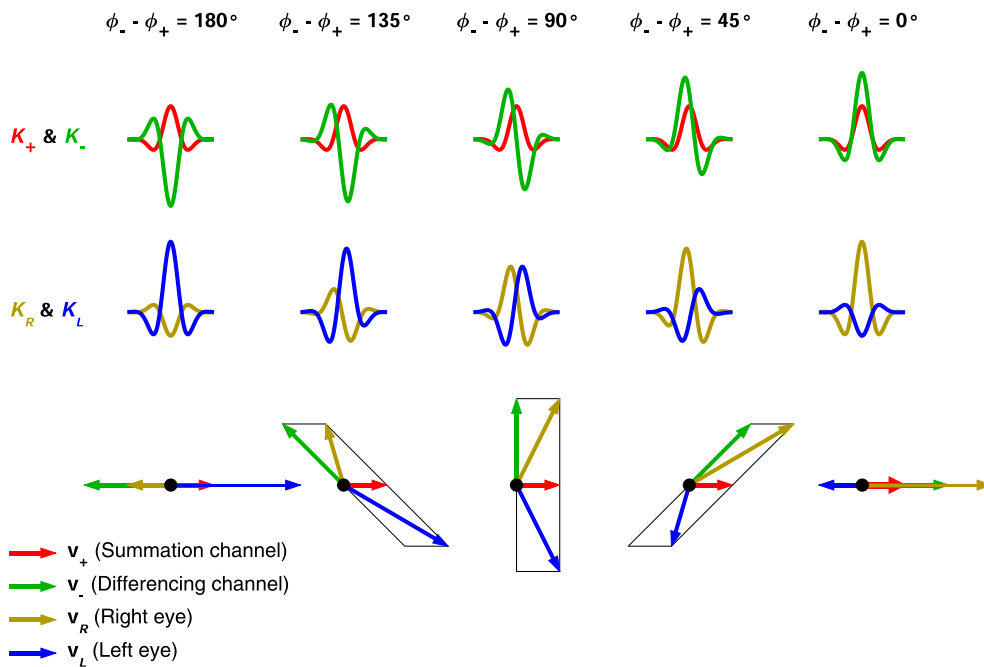


Fig. 4. The same as Fig. 3, but with $g_+/g_- = 1/2$. The longer v_- vector pulls v_L and v_R away from each other, so that the magnitude of the neuron's preferred binocular phase disparity, $|\phi_L - \phi_R|$, is greater than 90° in all cases, regardless of the values of ϕ_+ or ϕ_- .

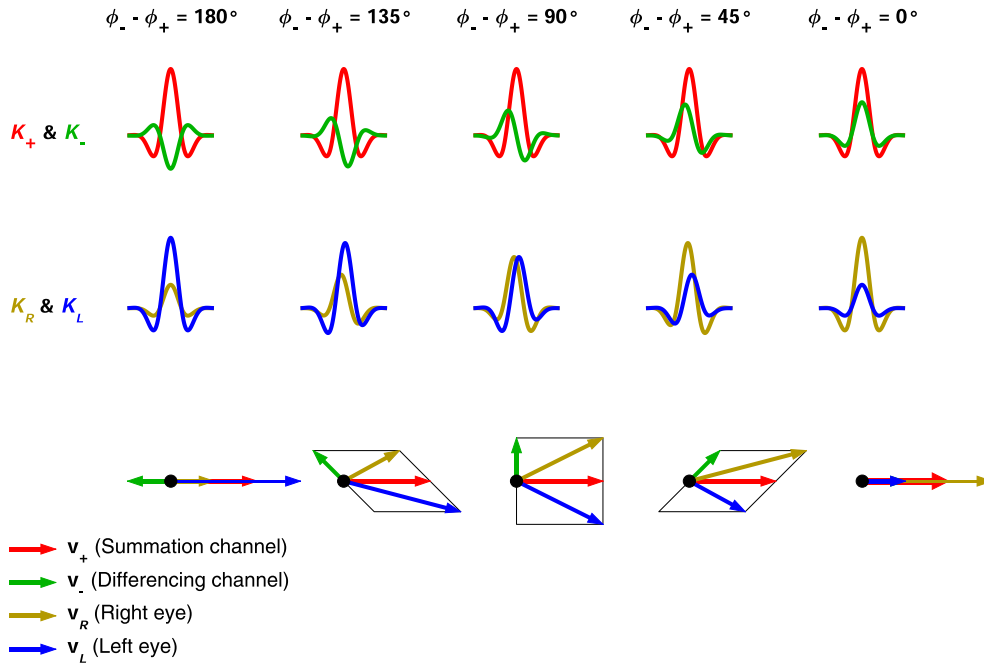


Fig. 5. The same as Fig. 3, but with $g_+/g_- = 2$. The longer v_+ vector pulls v_L and v_R towards each other, so that the magnitude of the neuron's preferred binocular phase disparity, $|\phi_L - \phi_R|$, is less than 90° in all cases, regardless of the values of ϕ_+ or ϕ_- .

ϕ_+ and ϕ_- can be freely chosen to suit the computation at hand: all pairs of ϕ_+ and ϕ_- are equally optimal¹. However, we will soon see that, although the phases of $K_+(x)$ and $K_-(x)$ can be freely chosen, the phase disparity between $K_L(x)$ and $K_R(x)$ is constrained by the sensitivity ratio, g_+/g_- .

We can represent the sensitivity and phase of each receptive field using a 2-dimensional vector, where the length of the vector represents the sensitivity, and the direction of the vector represents the phase (see the examples in Figs. 3–5). So let us define vector v_+ , for the summation channel, which has length $g_+/\sqrt{2}$ and angle ϕ_+ , and define vector v_- , for the differencing channel, which has length $g_-/\sqrt{2}$ and angle ϕ_- .

Having defined $K_+(x)$ and $K_-(x)$, we can obtain the neuron's right and left eye receptive fields. Using Eqs. (62) and (63) to substitute for $K_+(x)$ and $K_-(x)$ in Eq. (6), we have

$$K_R(x) = \frac{1}{\sqrt{2}} G(x) \left(\frac{g_+}{\sqrt{2}} \cos(2\pi f x + \phi_+) + \frac{g_-}{\sqrt{2}} \cos(2\pi f x + \phi_-) \right). \quad (64)$$

When adding together two sine waves of the same frequency, the result is a sine wave with the same frequency, but with amplitude and phase given by a vector that is the sum of the vectors representing the amplitudes and phases of the two sine waves being added together. Thus, we have

$$K_R(x) = \frac{g_R}{\sqrt{2}} G(x) \cos(2\pi f x + \phi_R), \quad (65)$$

where g_R and ϕ_R are the length and angle of vector $v_R = v_+ + v_-$. These are given by

$$g_R = \sqrt{\frac{g_+^2 + g_-^2 + 2g_+g_- \cos(\phi_- - \phi_+)}{2}} \quad (66)$$

¹ An explanation of this is beyond the scope of this article: it is possible to derive the full spatial receptive field using methods analogous to the derivation of the optimal ocular gains, and the free choice of phase values ϕ_+ and ϕ_- comes from a multiplexing step in which there is a range of equally optimal solutions.

$$\phi_R = \text{atan2}(g_+ \sin \phi_+ + g_- \sin \phi_-, g_+ \cos \phi_+ + g_- \cos \phi_-). \quad (67)$$

Similarly, using Eqs. (62) and (63) to substitute for $K_+(x)$ and $K_-(x)$ in Eq. (7), we have

$$K_L(x) = \frac{g_L}{\sqrt{2}} G(x) \cos(2\pi f x + \phi_L), \quad (68)$$

where g_L and ϕ_L are the length and angle of vector $v_L = v_+ - v_-$, i.e.

$$g_L = \sqrt{\frac{g_+^2 + g_-^2 - 2g_+g_- \cos(\phi_- - \phi_+)}{2}} \quad (69)$$

$$\phi_L = \text{atan2}(g_+ \sin \phi_+ - g_- \sin \phi_-, g_+ \cos \phi_+ - g_- \cos \phi_-). \quad (70)$$

The magnitude of the neuron's binocular phase disparity, $|\phi_L - \phi_R|$, can be calculated from Eqs. (67) and (70). Or alternatively from

$$|\phi_L - \phi_R| = \cos^{-1} \left(\frac{(g_+/g_-)^2 - 1}{\sqrt{[(g_+/g_-)^2 + 1]^2 - 4(g_+/g_-)^2 \cos^2(\phi_- - \phi_+)}} \right). \quad (71)$$

The sensitivities of the neuron's right and left eye receptive fields are given by $g_R/\sqrt{2}$ and $g_L/\sqrt{2}$, respectively. Figs. 3–5 illustrate $K_+(x)$, $K_-(x)$, $K_L(x)$ and $K_R(x)$ of some example model neurons, along with the corresponding vectors, v_+ , v_- , v_L and v_R .

As noted earlier, to fully represent the information in the two eyes, we need two output channels. Eqs. (57) and (58) show that these two channels are identical apart from the sign of the multiplier applied to the difference signal. The neuron outlined above implements one of these channels; to implement the other channel, we need a neuron with receptive fields $K'_+(x)$ and $K'_-(x)$ given by

$$K'_+(x) = K_+(x) \quad (72)$$

$$K'_-(x) = -K_-(x). \quad (73)$$

Using Eqs. (6) and (7), we can show that this second neuron's right and

left eye receptive fields, $K'_R(x)$ and $K'_L(x)$, are given by

$$K'_R(x) = K_L(x) \quad (74)$$

$$K'_L(x) = K_R(x). \quad (75)$$

In summary, we can have a range of equally optimal neurons with different ϕ_+ and ϕ_- ; however, for each of these neurons, there needs to be another neuron that is identical except that the left and right eye receptive fields are swapped between the eyes.

4. Relationships between neuronal parameters

The linear neuronal receptive field model outlined in the previous section gives rise to several relationships between the different neuronal parameters. These relationships can help us to use Li and Atick's theory to explain various physiological findings, and to make predictions that have not yet been tested.

4.1. Effect of $(\phi_- - \phi_+)$ and sensitivity ratio g_+/g_- on the neuron's preferred binocular disparity

Figs. 3–5 illustrate how the relative sensitivity of $K_+(x)$ versus $K_-(x)$ (i.e. g_+/g_-) constrains the neuron's preferred binocular disparity, $\phi_L - \phi_R$, i.e. the phase difference between $K_L(x)$ and $K_R(x)$:

1. When $g_+/g_- = 1$ (Fig. 3), the left and right eye kernels have a phase disparity of exactly 90° ; this is because in this case, the identical parallelograms formed by the vector addition and subtraction are rhombuses, so the diagonals (on which v_L and v_R lie) are orthogonal.
2. When $g_+/g_- < 1$ (Fig. 4), the left and right eye kernels have a phase disparity $> 90^\circ$; this is because the longer v_- vector pulls v_L and v_R away from each other.

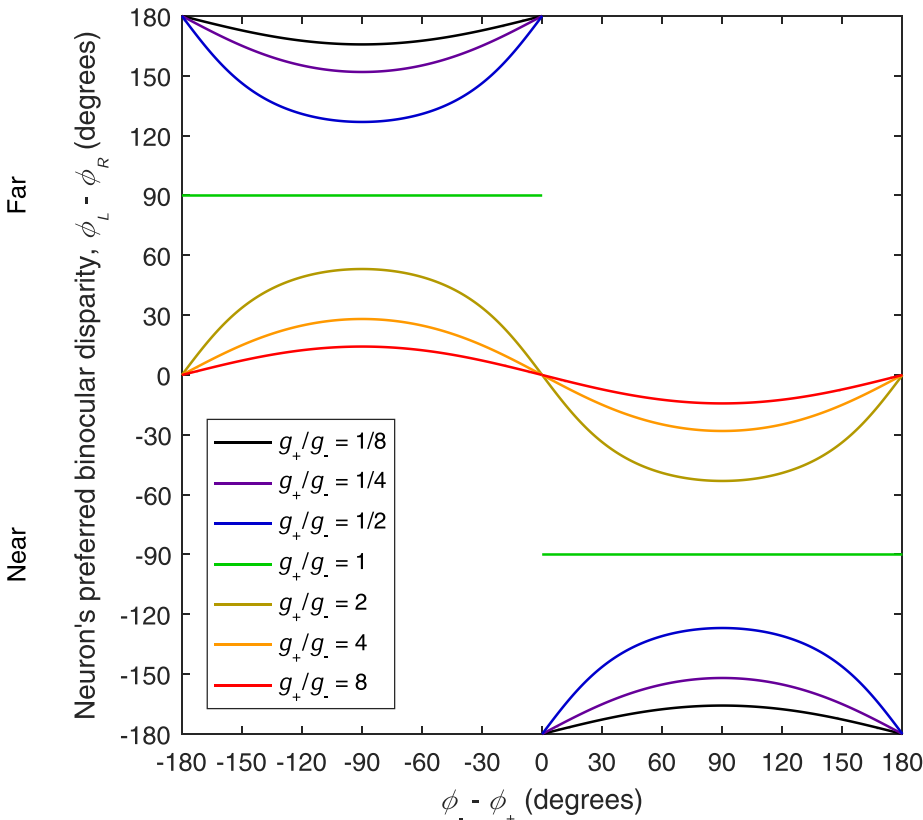


Fig. 6. This figure shows how the neuron's preferred binocular disparity, $\phi_L - \phi_R$, is affected by the sensitivity ratio, g_+/g_- , and the phase difference, $\phi_- - \phi_+$, of the summation and differencing channels. Binocular disparity was calculated using Eqs. (67) and (70). Fig. 4 illustrates parameter values that lie on the blue line ($g_+/g_- = 1/2$); Fig. 3 illustrates parameter values that lie on the green line ($g_+/g_- = 1$); Fig. 5 illustrates parameter values that lie on the yellow line ($g_+/g_- = 2$). Note, for this neuron, positive values of $\phi_- - \phi_+$ tune the neuron to near disparities, while negative values of $\phi_- - \phi_+$ tune the neuron to far disparities; if we had instead used the neuron defined by Eqs. (72) to (75), then the receptive fields would have been swapped between the eyes, and all the signs of the binocular disparities in this figure would have been reversed. (For interpretation of the references to colour in this figure legend, the reader is referred to the web version of this article.)

3. When $g_+/g_- > 1$ (Fig. 5), the left and right eye kernels have a phase disparity $< 90^\circ$; this is because the longer v_+ vector pulls v_L and v_R towards each other.

These constraints apply regardless of the phase values ϕ_+ and ϕ_- . Fig. 6 shows how $\phi_L - \phi_R$ varies with $\phi_- - \phi_+$ for several different values of g_+/g_- . Although g_+/g_- is imposed on the system by the signal and noise levels, ϕ_+ and ϕ_- can be freely chosen; Fig. 6 shows that, within the constraints outlined above, there is some scope to vary ϕ_+ and ϕ_- to yield a range of binocular phase disparities.

An alternative visualisation is given in Fig. 7. The shaded regions indicate the possible combinations of g_+/g_- and binocular disparity magnitude, $|\phi_L - \phi_R|$; for $g_+/g_- < 1$, only binocular disparities greater than 90° are possible, while for $g_+/g_- > 1$, only binocular disparities less than 90° are possible. The colour at each point in Fig. 7 indicates how much $|\phi_- - \phi_+|$ deviates from 90° (quadrature phase): the black end of the colour scale indicates that $K_+(x)$ and $K_-(x)$ are in quadrature phase ($|\phi_- - \phi_+| - 90^\circ = 0^\circ$), while the yellow end of the scale indicates that $K_+(x)$ and $K_-(x)$ are either exactly in phase or exactly out of phase ($|\phi_- - \phi_+| - 90^\circ = 90^\circ$). The curved boundaries of the shaded regions are lined with black, indicating that, as $K_+(x)$ and $K_-(x)$ approach quadrature phase, $|\phi_L - \phi_R|$ gets as close as possible to 90° . As $K_+(x)$ and $K_-(x)$ deviate from quadrature phase (i.e. become either in or out of phase), the left and right eye kernels become more out of phase for $g_+/g_- < 1$, and become more in phase for $g_+/g_- > 1$. The central point where the two shaded regions in Fig. 7 meet (corresponding to $g_+/g_- = 1$) represents the degenerate case where the left and right eye kernels are always in quadrature phase, i.e. $|\phi_L - \phi_R| = 90^\circ$, regardless of the values of ϕ_+ and ϕ_- .

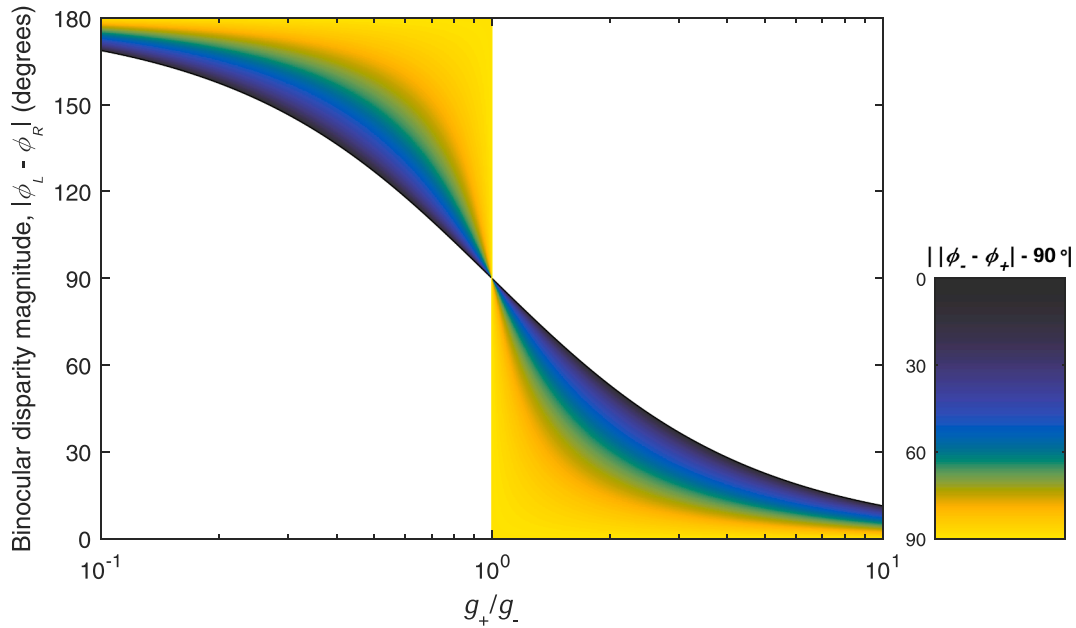


Fig. 7. The shaded areas show the possible combinations of g_+/g_- and preferred binocular disparity magnitude, $|\phi_L - \phi_R|$. This figure allows us to see at a glance that low g_+/g_- causes the neuron to be tuned to high binocular disparity, and high g_+/g_- causes preference for low binocular disparity. The colour at each shaded point indicates how much $|\phi_- - \phi_+|$ deviates from 90° (quadrature phase). Eq. (71) was rearranged to find the value of $|\phi_- - \phi_+|$ at each point.

4.2. Effect of $(\phi_- - \phi_+)$ and sensitivity ratio g_+/g_- on binocularity

Both the sensitivity ratio, g_+/g_- , and the phase difference, $\phi_- - \phi_+$, of the summation and differencing channels will affect the neuron's binocularity, i.e. the extent to which it is similarly sensitive to the two eyes. Binocularity can be assessed by presenting each eye with the optimal sine wave grating stimulus for that eye's receptive field, and then measuring the neuron's outputs, O_L and O_R , in response to left and right eye monocular stimulation, respectively. Binocularity can then be quantified using the Ocular Balance Index (OBI):

$$OBI = 1 - \frac{|O_R - O_L|}{|O_R + O_L|}. \quad (76)$$

The OBI varies from 0 (totally monocular – the neuron only responds to stimulation in one eye) to 1 (totally binocular – the neuron responds with equal strength to stimulation in either eye).

We can derive an analytical expression that gives the OBI as a function of g_+/g_- , and $\phi_- - \phi_+$. To simplify the mathematics, instead of using Gabor receptive fields with a Gaussian envelope, we will assume the envelope to be rectangular, with width equal to a whole number of

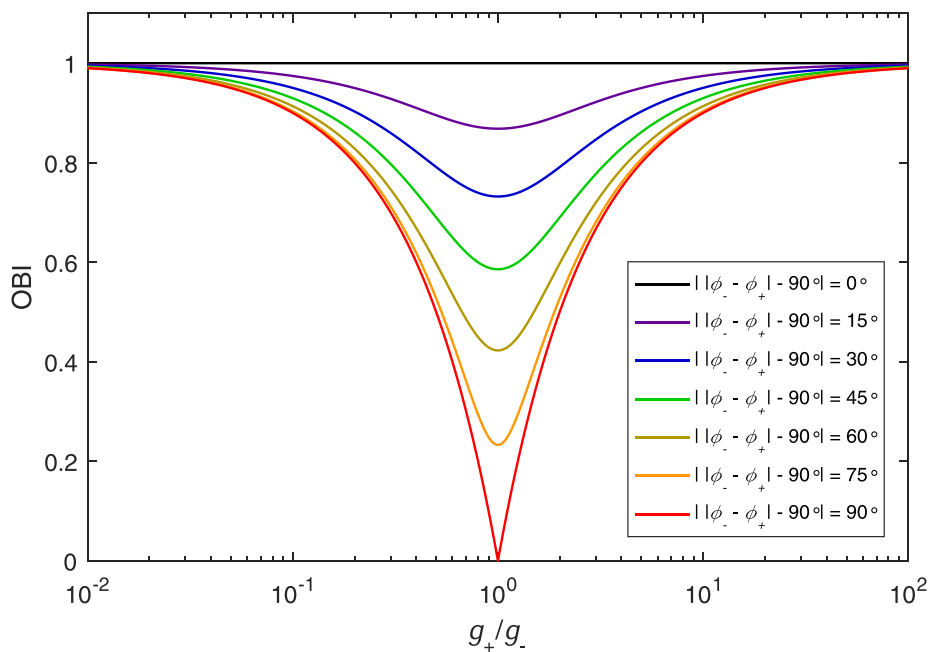


Fig. 8. Ocular Balance Index (OBI) plotted as a function of g_+/g_- , for several different values of $\phi_- - \phi_+$. The OBI is calculated using Eq. (76) with O_R and O_L given by Eqs. (79) and (80).

cycles of the carrier. We have carried out numerical modelling with biologically plausible Gabor functions, and found that using a rectangular envelope instead of a Gaussian makes a negligible difference to the predicted *OBI*.

If each receptive field is a whole number of cycles of a sine wave, then the neuron's response to the optimal sine wave stimulus will simply be proportional to the receptive field's sensitivity, so we have

$$O_R \propto g_R \quad (77)$$

$$O_L \propto g_L. \quad (78)$$

The actual constant of proportionality does not matter, since it will cancel out in Eq. (76). If we choose the constant of proportionality to be $\sqrt{2}/g_-$, then, using Eqs. (66) and (69) to substitute for g_R and g_L in (77) and (78), we have

$$O_R = \sqrt{(g_+/g_-)^2 + 1 + 2(g_+/g_-)\cos(\phi_- - \phi_+)} \quad (79)$$

$$O_L = \sqrt{(g_+/g_-)^2 + 1 - 2(g_+/g_-)\cos(\phi_- - \phi_+)}. \quad (80)$$

Fig. 8 plots the *OBI* as a function of g_+/g_- with O_R and O_L given by Eqs. (79) and (80). This figure illustrates two key effects:

1. For a given g_+/g_- , binocularity is maximised when $K_+(x)$ and $K_-(x)$ are in quadrature phase ($|\phi_- - \phi_+| - 90^\circ| = 0^\circ$), and minimised when their phase difference is 0° or 180° ($|\phi_- - \phi_+| - 90^\circ| = 90^\circ$). To understand why this happens, first consider the case of $K_+(x)$ and $K_-(x)$ perfectly in phase (a phase difference of 0°); this case maximises the amplitude of their sum, and minimises the amplitude of their difference, so $K_R(x)$ and $K_L(x)$ are maximally different in sensitivity. Alternatively, a phase difference of 180° between $K_+(x)$ and $K_-(x)$ minimises the amplitude of their sum, and maximises the amplitude of their difference, so $K_R(x)$ and $K_L(x)$ are again maximally different in sensitivity. Halfway between these two extremes (quadrature phase), the difference between $K_R(x)$ and $K_L(x)$ is minimised.
2. For a given phase difference, $\phi_- - \phi_+$, binocularity is minimised when $g_+/g_- = 1$. This is because, when $g_+/g_- = 1$, $K_+(x)$ and $K_-(x)$ have the

same amplitude, allowing for more complete cancellation when they are added or subtracted (depending on their phase difference); this minimises the sensitivity of either $K_R(x)$ or $K_L(x)$, making the neuron as monocular as possible.

For further insights into these effects, see Supplementary Appendix B.

Each point in Fig. 7 gives rise to a single value for each of g_+/g_- and $|\phi_- - \phi_+| - 90^\circ|$, and thus a single *OBI* value (since the *OBI* is determined only by these two values – see Fig. 8). These *OBI* values are plotted in Fig. 9. The *OBI* is highest when $|\phi_- - \phi_+|$ is as close as possible to 90° , because that is when $|\phi_- - \phi_+| = 90^\circ$ (see Fig. 7) which gives *OBI* = 1 in all cases. The *OBI* is also high when g_+/g_- takes an extreme (low or high) value.

The predicted *OBI* values in Figs. 8 and 9 are calculated assuming that the neuron is completely linear, as in Eq. (1). As noted earlier, to obtain the spike rate from a real neuron, the calculation of Eq. (1) is followed by subtraction of a threshold ≥ 0 , and then all negative values are set to zero (half wave rectification). The half wave rectification on its own makes no difference to the *OBI* because, for monocular stimulation with each eye's optimally positioned sine wave grating stimulus, Eq. (1) will always produce a positive number. However, the subtraction of a threshold in combination with half wave rectification can make the neuron appear much more monocular than it really is, and this would reduce the measured *OBI*. Ohzawa and Freeman (1986) showed that some neurons appeared very monocular when tested with monocular stimulation in each eye, but nevertheless showed strong interactions between the two eyes' stimuli when stimulated binocularly; they showed that this behaviour could be explained by including subtraction of a threshold in the linear model. An asymmetry between on responses and off responses could also reduce the *OBI*, particularly in cells with $g_- \gg g_+$. For more discussion of the effects of nonlinearities on the predictions of Li and Atick's theory, see Zhaoping (2014), Section 3.5.7.1.

5. Evaluating the predictions of the theory

The core of Li and Atick's theory is the predicted effect of SNR on the gains on the summation and differencing channels. We can therefore test the theory by looking at different situations that would be expected to

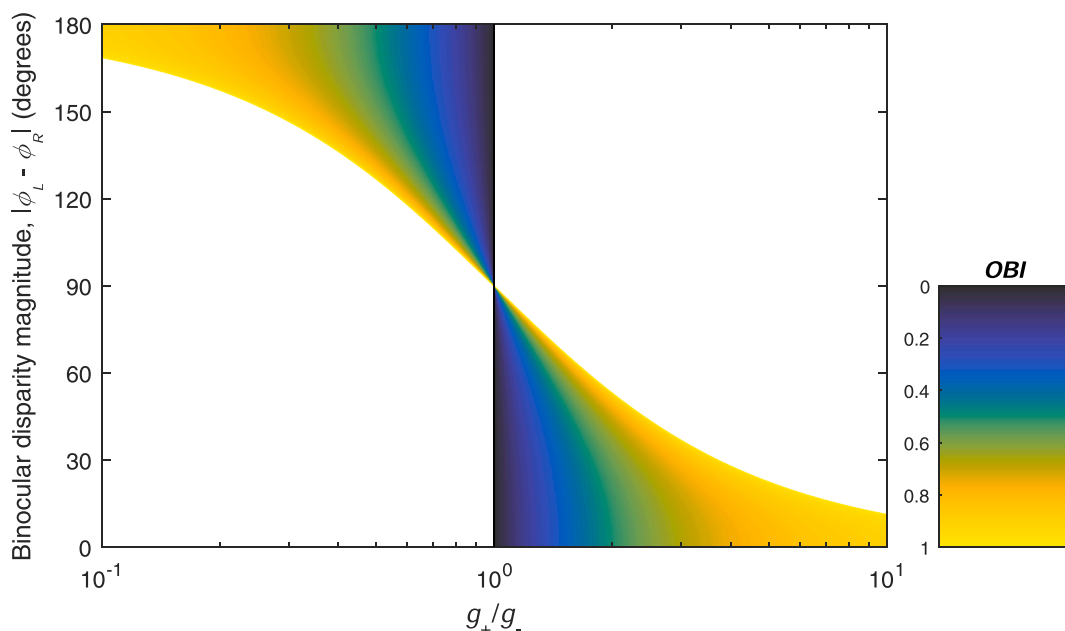


Fig. 9. Similar to Fig. 7, except that the colour of each point gives the *OBI* corresponding to each combination of g_+/g_- and $|\phi_L - \phi_R|$.

affect the channel gains, and seeing whether we get the predicted effects.

5.1. Predicted effects of interocular correlation on binocularity

Fig. 1 illustrates that, when the interocular correlation is zero, the signal strength is identical in the summation and differencing channels, i.e. $\langle S_+^2 \rangle = \langle S_-^2 \rangle$; since the optimal gain on each channel is determined by the SNR, a zero interocular correlation gives the same optimal gain on each channel, i.e. $g_+/g_- = 1$. When the interocular correlation is above zero, we have $\langle S_+^2 \rangle > \langle S_-^2 \rangle$. Although a pair of different SNRs can give rise to the same optimal gain on each channel, it is generally the case that different SNRs will give rise to different gains (see Fig. 2). Thus, in general, Li and Atick's theory predicts that, as the interocular correlation decreases, g_+/g_- will get closer to 1, and this in turn will make the neurons more monocular (as shown in Fig. 8); conversely, when the interocular correlation increases, g_+/g_- will move away from 1, and the neurons will be more binocular. The following subsections examine various factors that affect the interocular correlation, and show how they lead to the predicted effects on binocularity.

5.1.1. Strabismus (squint)

In strabismus, the eyes are not correctly aligned. This gives rise to a lower interocular correlation than normal, so Li and Atick's theory predicts a higher-than-normal level of monocularity. This prediction was confirmed by Hubel and Wiesel's (1965) finding that, in primary visual cortex of kittens raised with artificially induced strabismus, 79% of the neurons (302 of 384) were monocular, compared with 20% (44 of 223) in normally reared kittens (a significant difference in proportion: $\chi^2 = 199.8, p = 2.3 \times 10^{-45}$).

5.1.2. Alternating monocular occlusion

Strabismus reduces the interocular correlation, but does not abolish it completely. In addition to their experiments on artificially induced strabismus, Hubel and Wiesel (1965) raised kittens with daily alternating monocular occlusion, so that on each day, one eye was occluded with an opaque occluder, and the other eye was normal; the occluder was swapped between the eyes each day. In this setup, the occluded eye never had a signal – only noise – so the interocular correlation was zero at all times. Li and Atick's theory would therefore predict an even larger proportion of monocular cells than in strabismic animals; Hubel and Wiesel (1965) found that this was indeed the case: 91% of the neurons (176 of 194) that they recorded were monocular, a significantly higher proportion than for strabismic animals ($\chi^2 = 13.14, p = 0.00029$).

5.1.3. Interocular distance

Most primates have ocular dominance columns (ODCs), in which neurons are clustered according to which eye elicits the highest response (for review, see Adams & Horton, 2009). A strong ODC structure cannot occur without the existence of highly monocular neurons, i.e. those that respond mainly to one eye. ODCs are less readily observed in smaller primate species such as the owl monkey (Kaas, Ling, & Casagrande, 1976; Livingstone, 1996; Rowe, Benevento, & Rezak, 1978) squirrel monkey (Adams & Horton, 2003; Livingstone, 1996) and marmoset (Spatz, 1989). Although some studies have shown ODCs in these species (Adams & Horton, 2003; Chappert-Piquemal, Fonta, Malecaze, & Imbert, 2001; Takahata, Miyashita, Tanaka, & Kaas, 2014), the mixed findings suggest that these smaller species of primate show a weaker ocular dominance structure than shown by larger primates, such as macaques and humans. This is predicted by Li and Atick's theory, because the smaller primates have a shorter interocular distance (McCrea & Gdowski, 2003; Solomon & Rosa, 2014), leading to an increased interocular correlation; this should make the neurons less monocular, leading to a weaker ODC structure. Li and Atick's theory would predict that ODCs could be induced in these animals by introducing an artificial strabismus, thereby reducing the interocular

correlation, and making the neurons more monocular; this prediction has been confirmed in both the owl monkey and squirrel monkey (Livingstone, 1996).

5.1.4. Correlated electrical stimulation

Stryker and Strickland (1984) (see also Stryker (1986); Stryker (1989)) silenced the retinal ganglion cells of kittens by injecting tetrodotoxin into both eyes. Then, between the ages of 2 and 6–8 weeks, they applied electrical stimulation using a chronically implanted electrode in the optic tract; because the optic tract contains ganglion cell axons from both eyes, this created a very high correlation in the activity of cortical inputs from the two eyes. As predicted by Li and Atick's theory, this high interocular correlation resulted in more strongly binocular cells than in normally raised kittens.

5.1.5. Orientation

Because the two eyes are displaced horizontally rather than vertically, the binocular disparities are mainly horizontal shifts between the eyes. For a neuron with left and right eye receptive fields, the horizontal image components within the two receptive fields will differ less between the two eyes than the vertical image components. This causes the interocular correlation to be higher for horizontally than vertically oriented components (Li & Atick, 1994). Li and Atick's theory would therefore predict that horizontally tuned neurons should be more binocular than vertically tuned neurons. This prediction has been confirmed experimentally (see Zhaoping, 2014, Fig. 3.14).

5.2. Predicted effects of binocular adaptation

Viewing a distant scene will result in a high interocular correlation, while viewing objects at very close range will result in a lower interocular correlation. Thus, the optimal gains on the summation and differencing channels will change from moment to moment as we look around the visual environment. The system would therefore be expected to adapt quickly to changes in the prevailing interocular correlations. The next subsections review experiments that we have carried out to investigate the effects of adaptation on the gains of the summation and differencing channels.

5.2.1. A psychophysical paradigm that detects changes in gain ratio, g_+/g_-

The evidence outlined in Section 5.1 used indirect measurements of the ratio g_+/g_- : instead of measuring g_+/g_- directly, we looked at the level of binocularity, and used that to infer which condition had g_+/g_- closer to 1. About ten years ago, we devised a novel psychophysical paradigm to measure effects on g_+/g_- more directly. The basic idea is to create a dichoptic test stimulus that delivers identifiably different stimuli to the summation and differencing channels – for example, the two channels could receive different directions of motion (May, Zhaoping, & Hibbard, 2012), different orientations (May & Zhaoping, 2016), or even different face images (May & Zhaoping, 2019). So the summation channel receives one stimulus, S_+ , and the differencing channel receives a different stimulus, S_- . On each trial, we ask the participant to report whether they saw S_+ or S_- . The proportion of times they report S_+ is an index of the size of the ratio g_+/g_- .

To make the dichoptic test stimuli, it is easiest to begin with the desired S_+ and S_- , which could each be any spatiotemporal stimulus. Then we make one eye's stimulus (say the right eye) $S_R = (\alpha S_+ + \beta S_-)/2$, and the other eye's stimulus (say the left eye) $S_L = (\alpha S_+ - \beta S_-)/2$, where α and β are scalar multipliers that control the image contrast. The two eyes' stimuli then add together to give αS_+ , and subtract to give βS_- . In one study (May & Zhaoping, 2016), we had $\alpha = \beta$; in others (May & Zhaoping, 2019; May et al., 2012), we usually had $\alpha < \beta$ to compensate for a bias to perceive the binocular sum with foveal fixation (Zhaoping, 2017); this bias is thought to be nothing to do with gain control or efficient coding, instead being a bias in interpretation of the low-level signals by the subsequent perceptual decoding stage (see Zhaoping, 2017, for details).

To change the gain on each binocular channel, we present high-contrast adaptation stimuli that will strongly adapt either the summation channel or the differencing channel. To adapt the summation channel, we present the same adaptation stimulus in each eye (correlated adaptation), which gives a strong summation signal and a zero difference signal; to adapt the differencing channel, we reverse the contrast of the adaptation stimulus between the eyes (anticorrelated adaptation), so the difference signal is strong and the sum is zero. Because the adaptation stimuli are high-contrast (giving a high SNR), the predicted gains will vary inversely with the signal strength (see Fig. 2): anticorrelated adaptation should reduce sensitivity g_- to the binocular difference image, S_- , whereas correlated adaptation should reduce sensitivity g_+ to the binocular sum, S_+ . As predicted, we find that participants report seeing S_+ more frequently after anticorrelated than correlated adaptation (May & Zhaoping, 2016; May & Zhaoping, 2019; May et al., 2012).

In our first study with this paradigm (May et al., 2012), our dichoptic stimulus was based on that of Shadlen and Carney (1986). Each eye received a counterphase flickering grating; the binocular sum, S_+ , was a grating drifting smoothly in one direction, and the binocular difference, S_- , was a grating drifting in the opposite direction. In our second study (May & Zhaoping, 2016), the two eyes' stimuli were plaids, formed from the sum of two sine wave gratings tilted clockwise or anticlockwise of vertical; S_+ was a grating tilted in one direction, and S_- was a grating tilted in the opposite direction. There is a formal equivalence between these two studies because a moving grating is tilted in space-time (Adelson & Bergen, 1985), and each eye's plaid stimulus in our second study is essentially a space-time plot of the counterphase grating that we used in the first study.

These experiments deliberately did not adapt the perceptual dimension being tested. When participants were asked to judge the direction of motion of the test stimulus (May et al., 2012), the adaptation stimuli were stationary. When participants were asked to judge the grating tilt (May & Zhaoping, 2016) or face identity (May & Zhaoping, 2019), the adaptation stimuli were untilted noise. Thus, the adaptation effects must have resulted from adaptation of the binocular channels, not adaptation of the perceptual mechanisms on which the judgements were being based.

Many studies of perceptual aftereffects of adaptation are plagued by a fundamental difficulty: response bias can have effects indistinguishable from a genuine perceptual bias (Morgan, Dillenburger, Raphael, & Solomon, 2012). This is particularly problematic when the participant can see which adaptation condition they are currently in, and may be able to guess which response the experimenter is expecting them to make on each trial. Our paradigm does not suffer this problem. To understand why, consider our first study (May et al., 2012). Within each session, there were two types of trials, randomly interleaved: on one type of trial, S_+ had upward motion and S_- had downward motion; on the other type of trial, it was the other way round. This meant that any bias to respond "upward" or "downward" would have pushed performance towards chance, weakening the measured effect of adaptation. In summary, we could be certain that any measured effects of adaptation in our paradigm were due to adaptation of the binocular channels, and not a response bias or adaptation of the mechanisms on which the perceptual judgements were being based.

Because these adaptation effects were unequivocally due to adaptation of the binocular channels, we were able to use this paradigm to answer a long-standing question about whether face adaptation inherits adaptation from earlier stages in the processing stream, as argued by some researchers (Dickinson & Badcock, 2013; Dickinson, Almeida, Bell, & Badcock, 2010; Dickinson, Mighall, Almeida, Bell, & Badcock, 2012). This had always been a plausible idea, but the evidence for it was uncertain because all existing face aftereffects could conceivably have resulted from selective adaptation of the face processing mechanisms themselves (see May & Zhaoping, 2019 for a discussion of these issues). In our most recent study using this paradigm (May & Zhaoping, 2019), the S_+ and S_- stimuli were face images. For example, in one experiment,

half the trials had Brad Pitt as the S_+ stimulus and Matt Damon as the S_- stimulus; on the other half of trials, it was the other way round. We found that we could bias which face the participant perceived by selectively adapting the binocular channels using random noise stimuli that could not conceivably have selectively adapted the face processing mechanisms. This therefore provided the first completely conclusive evidence that face processing mechanisms can inherit adaptation from earlier processing stages.

5.2.2. Effects of adaptation on perceived depth

Elsewhere in this Special Issue, Kingdom, Yared, Hibbard, and May (2020) report the effects of correlated and anticorrelated adaptation on perceived depth. As shown in Figs. 6 and 7, the neuron's preferred binocular disparity decreases as g_+/g_- increases. Thus, after correlated adaptation (which reduces g_+/g_-), neurons would be tuned to larger disparities than normal, whereas, after anticorrelated adaptation (which increases g_+/g_-), neurons would be tuned to smaller disparities than normal. If the change in the neuron's preferred binocular disparity were the only effect of adaptation, one might expect perceived depth to be decreased after correlated adaptation because, post-adaptation, the neuron best tuned to the test stimulus disparity would be one that normally prefers smaller disparities; conversely one might expect perceived depth to be increased after anticorrelated adaptation because post-adaptation, the neuron best tuned to the test stimulus disparity would be one that normally prefers larger disparities. However, there is another effect at play. Correlated adaptation tends to reduce the sensitivity of neurons tuned to small disparities (since they are dominated by the summation channel), whereas anticorrelated adaptation tends to reduce the sensitivity of neurons tuned to large disparities (since they are dominated by the differencing channel). Thus, after correlated adaptation, the neurons tuned to large disparities would be more sensitive than those tuned to small disparities, which would tend to increase perceived depth; conversely, after anticorrelated adaptation, the neurons tuned to small disparities would be more sensitive than those tuned to large disparities, which would tend to decrease perceived depth. In summary, binocular adaptation has predicted effects on sensitivity and disparity tuning that work in opposite directions for depth perception. Kingdom et al. (2020) carried out modelling that showed that the effects on sensitivity would dominate; as predicted by the modelling, they found that perceived depth is increased after correlated binocular adaptation and reduced after anticorrelated adaptation.

6. Discussion

It is important to understand that Li and Atick's theory does not propose a novel neuronal architecture: the neuronal model that it uses, outlined in Eq. (1), is the standard model of a linear binocular simple cell, which has considerable empirical support (Ohzawa & Freeman, 1986). The novelty is in how this model is *described*, or *conceptualised*. It is conventional to describe the neuron in terms of its left and right eye receptive fields, $K_L(x)$ and $K_R(x)$, so that we can calculate its response directly from the left and right eye images (as in Eq. (1)); Li and Atick instead describe the neuron in terms of its binocular sum and difference receptive fields, $K_+(x)$ and $K_-(x)$, so that we can calculate its response directly from the sum and difference of the left and right eye images (as in Eq. (4)). This is analogous to the way in which we can switch between describing a simple cell in terms of its receptive field and describing it in terms of its spatial frequency tuning function (i.e., the Fourier transform of the receptive field): again, these are just two different descriptions of the same model, and if we know one description, we can derive the other (see Fig. 9 of Movshon, Thompson, & Tolhurst, 1978). This is a strong analogy because, for a particular point, x , in the image, the ordered pair $(K_+(x), K_-(x))$ is the discrete Fourier transform of $(K_L(x), K_R(x))$. Thus, the relationship between $(K_+(x), K_-(x))$ and $(K_L(x), K_R(x))$ is the same as the relationship between the spatial frequency tuning function and the receptive field (in both cases, one is the Fourier transform of the other).

The reason for describing the neuron in terms of $K_+(x)$ and $K_-(x)$ is that it helps us to understand how the parameters of the neuronal model are optimised. By conceptually switching from left and right eye channels to binocular summation and differencing channels, we move from a pair of (usually) correlated channels to a pair of uncorrelated channels. This greatly simplifies the optimisation process, because the optimal gains of the summation and differencing channels (g_+ and g_- , respectively) can be calculated independently of each other (using Eq. (44)). Once the optimal gains have been applied to the summation and differencing channels, Li and Atick propose a further transformation to produce two output channels that both have the same sensitivity to the binocular sum, and both have the same sensitivity to the binocular difference (the two output channels differ only in the sign of their response to the binocular difference – see Eqs. (57) and (58)). There are therefore three conceptually separate steps: decorrelation, gain control, and multiplexing.

To implement this process, the three steps can be cascaded into a single linear transformation that gives the sensitivity of each output channel to the binocular sum and difference (Eqs. (57) and (58)). Each of the two output channels would be implemented by a neuron. The amplitudes of its $K_+(x)$ and $K_-(x)$ receptive fields are the $g_+/\sqrt{2}$ and $g_-/\sqrt{2}$ terms in Eq. (57) or (58); the phases of $K_+(x)$ and $K_-(x)$ (ϕ_+ and ϕ_-) can be freely chosen to suit the task that the neuron will be used for. The neuron's right and left eye receptive fields are found simply by adding and subtracting $K_+(x)$ and $K_-(x)$ (see Eqs. (6) and (7)). As mentioned above, there are two output channels. They are implemented with two neurons with identical $K_+(x)$ but opposite-sign $K_-(x)$; the two neurons have the same pair of left and right eye receptive fields, but they differ in terms of which eye has which receptive field.

We have presented the theory as involving just a single pair neurons, because that is what is needed to represent the signals coming from the same retinal position in two eyes. In reality, there would be a whole range of different pairs of neurons, with different retinal positions, and also different receptive field characteristics, such as spatial frequency tuning and phases, ϕ_+ and ϕ_- . To allow accurate decoding of stimulus properties such as spatial frequency or binocular disparity, we need a population of neurons tuned to different values of these properties (Jazayeri & Movshon, 2006; Kingdom et al., 2020; May & Solomon, 2015).

A neuron's preferred binocular disparity and level of binocularity are both functions of just two variables: the gain ratio g_+/g_- , and the extent to which $|\phi_+ - \phi_-|$ differs from 90° (see Figs. 7 and 8). Since ϕ_+ and ϕ_- can be freely chosen, Li and Atick's theory cannot make strong predictions that depend on $|\phi_+ - \phi_-|$; the core of the theory is the predicted gain values, g_+ and g_- .

Fig. 1 shows that, when the interocular correlation is low, the binocular summation and differencing channels will have similar SNR. Since the optimal gain is a function of the SNR (Fig. 2), Li and Atick's theory predicts that, as the interocular correlation approaches zero, the gain ratio g_+/g_- approaches 1, and the neurons will become as monocular as possible (see Fig. 8). In Section 5.1, we describe several examples where a manipulation of interocular correlation has been shown to result in the predicted effect on binocularity.

It is less easy to predict binocular disparity tuning. When the interocular correlation is low, g_+/g_- is close to 1, and in this vicinity, the theory predicts that the preferred binocular disparity can take any value (see Fig. 7 or Fig. 9). When the interocular correlation is high, the optimal g_+ and g_- will usually differ substantially but, depending on the SNR, g_+/g_- may be above 1 (which predicts a low preferred binocular disparity), or below 1 (which predicts a high preferred binocular disparity).

For much of this article, we have presented the binocular summation and differencing channels as abstract, conceptual devices that allow us to derive the optimal binocular coding strategy. In general, these channels are not separated into different neuronal pathways: most neurons will carry signals from both channels (multiplexing). Theoretically, these channels should act like classical psychophysical channels, in the sense of

functionally independent mechanisms that process different aspects of the stimulus and are selectively adaptable (Mollon, 1974). To maintain optimal coding, the channels should adapt as the interocular correlation or luminance level changes, as these changes will both affect the optimal channel gains. Since the two channels are in general multiplexed on a single neuron, selective adaptation of one channel will affect not just the neuron's sensitivity, but also its receptive field structure and its preferred binocular disparity (see Fig. 1 of Kingdom et al., 2020).

Empirically, we have shown that these channels are indeed selectively adaptable. In our adaptation experiments, we used binocular adaptation stimuli that selectively stimulated either the summation or differencing channel, but could not cause selective adaptation of the perceptual dimension being tested: perceived motion direction was affected by adaptation to static stimuli (May et al., 2012), perceived tilt direction was affected by adaptation to untilted stimuli (May & Zhaoping, 2016), perceived depth was affected by adaptation to stimuli containing no depth (Kingdom et al., 2020), and perceived human face was affected by adaptation to random noise (May & Zhaoping, 2019). Since our adaptation effects cannot be explained by adaptation of the mechanisms processing the perceptual dimension being tested, that leaves selective adaptation of the binocular summation or differencing channel as the only explanation of these counterintuitive adaptation effects.

CRedit authorship contribution statement

Keith May: Software, Visualization, Writing – original draft, Writing - review & editing. **Li Zhaoping:** Conceptualization, Writing - review & editing.

Acknowledgements

Li Zhaoping is funded by the University of Tübingen and Max Planck Society.

Appendix A. Supplementary data

Supplementary data to this article can be found online at <https://doi.org/10.1016/j.visres.2021.08.005>.

References

- Adams, D. L., & Horton, J. C. (2003). Capricious expression of cortical columns in the primate brain. *Nature Neuroscience*, 6(2), 113–114. <https://doi.org/10.1038/nn1004>
- Adams, D. L., & Horton, J. C. (2009). Ocular dominance columns: Enigmas and challenges. *The Neuroscientist*, 15(1), 62–77. <https://doi.org/10.1177/1073858408327806>
- Adelson, E. H., & Bergen, J. R. (1985). Spatiotemporal energy models for the perception of motion. *Journal of the Optical Society of America, A*, 2(2), 284–299.
- Attneave, F. (1954). Some informational aspects of visual perception. *Psychological Review*, 61(3), 183–193.
- Barlow, H. B. (1961). Possible principles underlying the transformations of sensory messages. In W. A. Rosenblith (Ed.), *Sensory Communication*. Cambridge, MA: MIT Press.
- Barlow, H. (2001). Redundancy reduction revisited. *Network: Computation in Neural Systems*, 12(3), 241–253.
- Chappert-Piquemal, Catherine, Fonta, Caroline, Malecaze, François, & Imbert, Michel (2001). Ocular dominance columns in the adult New World Monkey Callithrix jacchus. *Visual Neuroscience*, 18(3), 407–412. <https://doi.org/10.1017/S0952523801183070>
- Dickinson, J., & Badcock, D. (2013). On the hierarchical inheritance of aftereffects in the visual system. *Frontiers in Psychology*, 4(472). <https://doi.org/10.3389/fpsyg.2013.00472>
- Dickinson, J. E., Almeida, R. A., Bell, J., & Badcock, D. R. (2010). Global shape aftereffects have a local substrate: A tilt aftereffect field. *Journal of Vision*, 10(13), 5, 1–12. <https://doi.org/10.1167/10.13.5>
- Dickinson, J. E., Mighall, H. K., Almeida, R. A., Bell, J., & Badcock, D. R. (2012). Rapidly acquired shape and face aftereffects are retinotopic and local in origin. *Vision Research*, 65, 1–11. <https://doi.org/10.1016/j.visres.2012.05.012>
- Hubel, D. H., & Wiesel, T. N. (1965). Binocular interaction in striate cortex of kittens reared with artificial squint. *Journal of Neurophysiology*, 28(6), 1041–1059. <https://doi.org/10.1152/jn.1965.28.6.1041>

- Jazayeri, M., & Movshon, J. A. (2006). Optimal representation of sensory information by neural populations. *Nature Neuroscience*, 9(5), 690–696. <https://doi.org/10.1038/nrn1691>
- Kaas, J. H., Ling, C.-S., & Casagrande, V. A. (1976). The relay of ipsilateral and contralateral retinal input from the lateral geniculate nucleus to striate cortex in the owl monkey: A transneuronal transport study. *Brain Research*, 106(2), 371–378. [https://doi.org/10.1016/0006-8993\(76\)91032-5](https://doi.org/10.1016/0006-8993(76)91032-5)
- Kingdom, F. A. A., Yared, K.-C., Hibbard, P. B., & May, K. A. (2020). Stereoscopic depth adaptation from binocularly correlated versus anti-correlated noise: Test of an efficient coding theory of stereopsis. *Vision Research*, 166, 60–71. <https://doi.org/10.1016/j.visres.2019.10.009>
- Li, Z., & Atick, J. J. (1994). Efficient stereo coding in the multiscale representation. *Network: Computation in Neural Systems*, 5, 157–174.
- Livingstone, M. S. (1996). Ocular dominance columns in New World monkeys. *The Journal of Neuroscience*, 16(6), 2086–2096. <https://doi.org/10.1523/JNEUROSCI.16-06-02086.1996>
- May, K. A., & Solomon, J. A. (2015). Connecting psychophysical performance to neuronal response properties I: Discrimination of suprathreshold stimuli. *Journal of Vision*, 15(6), 8. <https://doi.org/10.1167/15.6.8>
- May, K., & Zhaoping, L. (2016). Efficient coding theory predicts a tilt aftereffect from viewing untilted patterns. *Current Biology*, 26(12), 1571–1576. <https://doi.org/10.1016/j.cub.2016.04.037>
- May, K. A., & Zhaoping, L. (2019). Face perception inherits low-level binocular adaptation. *Journal of Vision*, 19(7):7, 1–10. <https://doi.org/10.1167/19.7.7>
- May, K., Zhaoping, L. i., & Hibbard, P. (2012). Perceived direction of motion determined by adaptation to static binocular images. *Current Biology*, 22(1), 28–32. <https://doi.org/10.1016/j.cub.2011.11.025>
- McCrea, R. A., & Gdowski, G. T. (2003). Firing behaviour of squirrel monkey eye movement-related vestibular nucleus neurons during gaze saccades. *The Journal of Physiology*, 546(1), 207–224. <https://doi.org/10.1113/jphysiol.2002.027797>
- Mollon, J. (1974). After-effects and the brain. *New Scientist*, 61, 479–482.
- Morgan, M., Dillenburger, B., Raphael, S., & Solomon, J. A. (2012). Observers can voluntarily shift their psychometric functions without losing sensitivity. *Attention, Perception, & Psychophysics*, 74(1), 185–193. <https://doi.org/10.3758/s13414-011-0222-7>
- Movshon, J. A., Thompson, I. D., & Tolhurst, D. J. (1978). Spatial summation in the receptive fields of simple cells in the cat's striate cortex. *Journal of Physiology*, 283, 53–77.
- Ohzawa, I., & Freeman, R. D. (1986). The binocular organization of simple cells in the cat's visual cortex. *Journal of Neurophysiology*, 56(1), 221–242. <https://doi.org/10.1152/jn.1986.56.1.221>
- Rowe, M. H., Benevento, L. A., & Rezak, M. (1978). Some observations on the patterns of segregated geniculate inputs to the visual cortex in New World primates: An autoradiographic study. *Brain Research*, 159(2), 371–378. [https://doi.org/10.1016/0006-8993\(78\)90542-5](https://doi.org/10.1016/0006-8993(78)90542-5)
- Shadlen, M., & Carney, T. (1986). Mechanisms of human motion perception revealed by a new cyclopean illusion. *Science*, 232(4746), 95–97.
- Solomon, S. G., & Rosa, M. G. P. (2014). A simpler primate brain: The visual system of the marmoset monkey. *Frontiers in Neural Circuits*, 8(96). <https://doi.org/10.3389/fncir.2014.00096>
- Spatz, W. B. (1989). Loss of ocular dominance columns with maturity in the monkey, *Callithrix jacchus*. *Brain Research*, 488(1), 376–380. [https://doi.org/10.1016/0006-8993\(89\)90734-8](https://doi.org/10.1016/0006-8993(89)90734-8)
- Stryker, M. P. (1986). The role of neural activity in rearranging connections in the central visual system. In R. J. Ruben, T. Van de Water, & E. W. Rubel (Eds.), *The biology of change in otolaryngology: Proceedings of the symposium of the 9th ARO Mid-winter Research Meeting "Biology of Change in Otolaryngology"* Clearwater Beach, FL, 2-6 February 1986 (pp. 211–224). Amsterdam: Elsevier B.V.
- Stryker, M. P. (1989). Evidence for possible role of spontaneous electrical activity in the development of the mammalian visual cortex. In P. Kellaway, & J. L. Noebels (Eds.), *Problems and Concepts in Developmental Neurophysiology* (pp. 110–130). Baltimore: Johns Hopkins University Press.
- Stryker, M. P., & Strickland, S. L. (1984). Physiological segregation of ocular dominance columns depends on the pattern of afferent electrical activity. *Investigative Ophthalmology & Visual Science (Supplement)*, 25, 278.
- Takahata, T., Miyashita, M., Tanaka, S., & Kaas, J. H. (2014). Identification of ocular dominance domains in New World owl monkeys by immediate-early gene expression. *Proceedings of the National Academy of Sciences*, 111(11), 4297–4302. <https://doi.org/10.1073/pnas.1401951111>
- Zhaoping, L. (2014). *Understanding Vision: Theory, Models, and Data*. Oxford: Oxford University Press.
- Zhaoping, L. (2017). Feedback from higher to lower visual areas for visual recognition may be weaker in the periphery: Glimpses from the perception of brief dichoptic stimuli. *Vision Research*, 136, 32–49. <https://doi.org/10.1016/j.visres.2017.05.002>